# FRACTURE MECHANICS EVALUATION OF A BOILING WATER REACTOR VESSEL FOLLOWING A POSTULATED LOSS OF COOLANT ACCIDENT

S. RANGANATH

*General Electric Co., Stress & Fracture Analysis Unit, Nuclear Energy Engineering Department, 175 Curtner Avenue, San Jose, California 95125, U.S.A.*

ABSTRACT

A fracture mechanics analysis is performed to evaluate the effects of a postulated Loss of Coolant Accident (LOCA) on the structural integrity of the pressure vessel in a Boiling Water Reactor. The LOCA event considered here is due to the postulated sudden rupture of the main steam line in a BWR. Several emergency core cooling systems are activated at different times after the LOCA and the vessel is flooded with cooling water. The vessel blowdown and the subsequent injection of cold water produces low temperature and high thermal stresses in the vessel. The temperature distribution and the resulting thermal stress in the vessel wall are determined using an axisymmetric finite element solution. The applied stress intensity factor is calculated as a function of crack depth for a postulated surface crack in the belt line region of the vessel wall for the combined thermal, pressure and residual stresses. The available toughness calculated as a function of crack tip temperature and fluence level, was significantly higher than the applied stress intensity factor at all times during the transient. It is, therefore, concluded that the pressure vessel will have a considerable margin to failure by brittle fracture even in the presence of large postulated initial flaws.

9110110105 911008
PDR ADOCK 05000387
Q PDR

## INTRODUCTION

The objective of this study is to assess the capability of General Electric Boiling Water Reactor (BWR) Pressure Vessels to withstand the consequences of a Design Basis Loss of Coolant Accident without compromising the structural integrity of the vessel. Following the postulated Loss of Coolant Accident (LOCA), the emergency core cooling systems are initiated. This results in the injection of large quantities of cold water into the reactor vessel causing thermal stress in the vessel wall. The determination of the thermal stresses in the vessel and a fracture mechanics evaluation of the vessel wall during the LOCA forms the subject matter of this paper. The analysis is performed for a 238 in. size BWR/6 pressure vessel. The focus of interest is the beltline region where the radiation effects are significant, and the potential consequence of a LOCA more severe than in other regions.

## 2. DESCRIPTION OF THE LOCA EVENT

A schematic picture of a typical BWR/6 vessel is shown in Figure 1. The pressure vessel is made of low alloy steel with stainless steel cladding and is subject to 1050 psig pressure and 552°F temperature under normal operating conditions. The vessel wall is separated from the core by an annulus which carries recirculation water and limits radiation damage to the vessel. Although the BWR/6 vessel comes in three sizes, 251 inch, 238 inch and 201 inch diameter, the structural details and operating conditions are similar. The present analysis is applicable for all three plant sizes.

In analyzing the LOCA event for a fracture evaluation, two types of pipe ruptures can be postulated; (i) steam line break, (ii) recirculation line break. Both events assume a guillotine rupture of the line when the reactor is operating at full power. Evaluation of the heat transfer conditions and temperature gradients showed that the steam line break is more severe than the recirculation line break from the viewpoint of thermal stresses and brittle fracture. Therefore, the steam line break is considered as the controlling design basis accident for the purpose of this evaluation.

Following the postulated guillotine rupture of the steam line, the reactor undergoes rapid depressurization during which two phase flow with boiling occurs. Immediately following the break, the large increase in core void fraction due to depressurization causes a sharp reduction in reactor power and control rod scram will be initiated in less than a second. Several Emergency Core Cooling Systems (ECCS) are activated following the pipe break. Figure 2 shows a representation of the variation of pressure, water temperature and water level in the vessel as a function of time after the pipe rupture. Immediately after the break there is rapid depressurization from 1050 psi to about 120 psi in approximately 1 minute. Following this there is a more gradual depressurization to ambient pressure at around 5 minutes after the pipe break. After this point, the pressure shows a slight increase. The coolant temperature follows the saturation temperature corresponding to the vessel pressure. After about 15 minutes, the pressure and the corresponding temperature start to decrease and reach ambient pressure at about an

hour after the pipe break. During the entire LOCA event the water level in the vessel stays well above the top of the active fuel zone. Therefore, the belt line region of the vessel which is being evaluated here is always surrounded by water on the inside surface.

3. THERMAL ANALYSIS OF THE PRESSURE VESSEL WALL IN THE BELT LINE REGION

The thermal conditions occurring in the vessel belt line region after this accident can be classified in two regimes:

Regime 1: Immediately after the accident and before the vessel coolant is subcooled by the ECCS flow, the reactor undergoes rapid depressurization. During this regime, the ECCS flows are not sufficiently subcooled to absorb the decay heat and sensible energy of the reactor assembly and coolant without vaporization. Therefore, boiling occurs at the interface between the vessel wall and the reactor coolant. As a result, the heat transfer regime is forced two-phase convection with boiling for which the heat transfer coefficient is potentially as high as 10,000 Btu/hr-ft$^2$ $^\circ$F.

Regime 2: Some time after all ECCS systems are initiated, the coolant flow is sufficient to subcool the bulk liquid inventory, and the flow regime is forced convection of subcooled water over a metal surface. The heat transfer coefficient could be as high as 500 Btu/hr-ft$^2$ $^\circ$F for this regime.

The assumed heat transfer conditions are conservative and are justified in Reference [1-2]. To add additional conservatism to the present analysis, it will be assumed Regime 1 exists during the entire depressurization period, (i.e., up to 300 seconds after the pipe break when the pressure reaches ambient conditions). After 300 seconds, the heat transfer coefficient is assumed to be 500 Btu/hr-ft$^2$ $^\circ$F for the remainder of the LOCA event. The outside surface of the vessel wall is covered by insulation. An effective heat transfer coefficient of 0.2 Btu/hr-ft$^2$ $^\circ$F is assumed for the outside surface and the bulk temperature of the drywell is assumed to the be 120$^\circ$F.

To confirm that the analytical results are not sensitive to the assumed heat transfer conditions, an additional case where the inside surface heat transfer coefficient was assumed to be 10,000 Btu/hr-ft$^2$ $^\circ$F for up to 1000 seconds after the LOCA was analyzed. This comparison showed that the changes in the calculated thermal stresses were small and that the assumptions of this analysis are still conservative.

Thermal analysis was performed using the finite element program ANSYS [3]. Transient thermal analysis was performed using an axisymmetric finite element model with isoparametric heat conduction elements with surface convection capability. Since the temperature distribution through the thickness of the vessel wall is expected to be independent of the axial location in the belt line region, only a small section of the vessel is selected for analysis.

The inside surface of the vessel wall is assumed to be clad with a 0.2-inch thick

layer of stainless steel. The base material of the wall is low alloy steel, SA533 Grade B, Class I and the overall wall thickness is six inches. Before the LOCA event, the vessel is assumed to be in steady state thermal equilibrium with the water at 550°F. After the LOCA the bulk water temperature follows the distribution in Figure 2, and the corresponding heat transfer coefficients apply. The temperature distribution through the wall thickness at different times during the LOCA event are shown in Figure 3. Because of the high surface heat transfer coefficient, the clad surface follows the bulk water temperature closely. However, since stainless steel has relatively lower thermal conductivity compared to the low alloy steel material of the wall, there is a significant temperature gradient in the clad. In other words, the clad protects the base material and reduces the thermal gradient in the vessel wall. The vessel responds to the temperature change very slowly and even after 300 seconds almost half of the wall thickness remains at temperatures exceeding 500°F. After 300 seconds the clad temperature starts going up and at the end of 1000 seconds the temperature of the clad is 300°F while the outside surface is at approximately 400°F.

## 4. STRESS ANALYSIS

### 4.1 Thermal Stresses

The finite element model used for stress analysis was the same as that used for thermal analysis. Isoparametric stress elements were used in place of the heat conduction elements. Temperature dependent properties were used for both the Young's Modulus and the coefficient of thermal expansion. Stress analysis was performed (assuming elastic behavior) at different selected times in the transient and the corresponding temperature distribution was provided on tape for stress analysis. The thermal stress distribution at different times during the transient are shown in Figure 4. Because of the differences in thermal expansion coefficients between the clad and base material, there is a discontinuity in the thermal stress at the interface. The thermal stresses reached the maximum value between 200-300 seconds. During this time interval, the changes were mainly in the stress distribution through the thickness. The overall maximum thermal stress occurred at about 300 seconds. This is reasonable since the coolant temperature shows a slight increasing trend after this point. Ultimately the vessel wall temperature reaches uniform condition and the thermal stresses become negligible.

### 4.2 Pressure Stresses

Pressure stresses are important only in the early part of the LOCA. Since the depressurization is rapid, there is little time for thermal stresses to be developed when the pressure stresses are still significant. However, when the thermal stresses are fully developed, the vessel pressure is small and the contribution of pressure stress to the overall stress state is negligible at this time.

### 4.3 Residual Stresses

The magnitude of the residual stress and its distribution in heavy welded sections

has been experimentally investigated in Reference [8]. The results indicated that the maximum residual stress in A302B welded sections after the stress relief at 1160±15°F did not exceed 8000 psi.

## 9. FRACTURE MECHANICS EVALUATION

In this section the stress intensity factor due to the applied stress is evaluated as a function of the postulated crack depth. The stress intensity calculations are performed at different times during the transient and the available toughness is determined corresponding to the temperature distribution at the same times. Effect of temperature and neutron fluence are included. The applied stress intensity factors are then compared with the available toughness to evaluate the brittle fracture safety margin.

### 9.1 Postulated Flaw

A surface flaw is assumed for this analysis since it is more limiting than a subsurface flaw of the same size. Also, since the thermal stress and the fluence are highest at the surface, the surface flaw will be subjected to more severe fracture conditions. The depth of the surface flaw includes the clad thickness although, the clad itself is austenitic stainless steel for which LEFM is not applicable. However, for crack depths exceeding the clad thickness, the crack tip is in the ferritic base material and brittle fracture concepts are appropriate for this case. The flaw shape considered for fracture analysis is a semi-elliptic surface flaw with a length to depth ratio of six. This flaw configuration is similar to that used in Appendix G, Section III of the ASME Code [5] for fracture mechanics evaluations.

### 9.2 Method of Evaluation of Stress Intensity Factors

The method of fracture evaluation used in this report is based on Linear Elastic Fracture Mechanics (LEFM). The essence of this approach is to perform an elastic evaluation of the stresses, calculate the elastic stress intensity factor at the crack tip and compare it with the material fracture toughness property. Although there is some yielding of the material during the LOCA, the yielding is mostly constrained by surrounding elastic material and the use of LEFM for this evaluation is appropriate.

Stress intensity solutions have been recommended in Section XI of the ASME Code [6] for finite semi-elliptic flaws subjected to membrane and bending stress distributions. For nonlinear stress distribution an approximate linearization technique is recommended. However, this is not adequate for handling the highly nonlinear thermal stress distribution that exists during a LOCA. Therefore, an alternate procedure which uses a polynomial fit to the actual stress distribution [7] and considers long continuous cracks is used in this analysis. This method, based on the superposition principle, consists of applying the stress distribution of the uncracked structure on the crack surface. For an arbitrary stress distribution represented by a third-degree polynomial:

$$\sigma(x) = A_0 + A_1x^2 + A_2x^2 + A_3x^3$$

in the uncracked section, the stress intensity factor for a continuous crack can be conveniently expressed as follows:

$$K_I = \sqrt{\pi a}\left[A_0F_1 + A_1F_2\left(\frac{2a}{\pi}\right) + A_2F_3\left(\frac{a^2}{2}\right) + A_3F_4\left(\frac{4a^3}{3\pi}\right)\right].$$

where the coefficients $F_1$, $F_2$, $F_3$ and $F_4$ are determined using finite element solutions. Reference [7] provides curves for the magnification factors $F_1$, $F_2$, $F_3$ and $F_4$ for continuous circumferential and longitudinal cracks in a cylindrical shell (t/R = 0.1). Since the flaw considered for evaluation is a finite length part-through flaw, it is conservative to use a stress intensity solution developed for a long continuous flaw in this analysis.

The magnification factors from Reference [7] were used in this analysis. The thickness to radius ratio for a BWR is smaller than that used in [7] but this difference is not expected to cause significant changes in the calculated stress intensity factor. The stress intensity factor for the discontinuous part of the stress in the clad was calculated separately using superposition of two uniform stress distributions of opposite signs.

5.3 Toughness Evaluation

The Reference Nil Ductility Transition Temperature ($RT_{NDT}$) of the vessel material is determined in accordance with the definition in NB-2300, Section III, ASME Code [5]. According to BWR/6 specifications, the $RT_{NDT}$ of the vessel shell material cannot exceed 10°F and the $RT_{NDT}$ of the weld metal used cannot be higher than -20°F. The basic material and the weld material for the core beltline region meets the following requirements:

a. The minimum upper shelf energy level, as determined by transverse and longitudinal Charpy-V notch impact specimens, shall be 75 ft lbs.

b. The maximum limits on copper and phosphorous content are 0.12% and 0.015% for the base material and 0.1% and 0.025% for the weld material respectively.

The maximum fluence levels in the core beltline region differ with the plant size. The 218-inch diameter BWR/6 vessel experiences the highest fluence level and is conservatively used for this evaluaton. The peak fluence level used in this evaluation considered the maximum values for both the axial and azimuthal fluence variation. The variation of fluence level through the thickness was included. The effect of neutron fluence on the fracture toughness of the vessel material can be measured by the shift in $RT_{NDT}$ with fluence. Section XI of the ASME Code [6] provides curves for the shift in $RT_{NDT}$ with fluence for different copper contents. However, more recently, the Nuclear Regulatory Commission has issued Regulatory Guide 1.99 [8] which predicts somewhat higher shift in $RT_{NDT}$ when compared with the code curves. For this analysis, the more conser-



6 1/

ative shift curves from Reference [8] were used. The adjustment to $RT_{NDT}$ for fluence s determined as a function of the maximum residual copper and phosphorous content and e local fluence level. The available toughness, $K_{IC}$ at any temperature T can then determined using the curves from Section XI of the ASME Code. An approximate equation r the fracture toughness curve of Section XI is:

$$K_{IC} = 33.2 + 2.806 \exp\left[.02\ (T-RT_{NDT} + 100^{\circ}F)\right]$$

ere the toughness $K_{IC}$ is in units of ksi $\sqrt{in.}$ and temperatures are in degrees Fahrenheit.

Knowing the crack tip temperature and the final $RT_{NDT}$ corresponding to the final luence level, the available toughness was calculated. The toughness curves in the code re abruptly cut off at 200 ksi $\sqrt{in}$ mainly because of the difficulty of measuring valid lane strain toughness data beyond this toughness value. For this analysis it will be sumed that the maximum available toughness is 200 ksi $\sqrt{in.}$

### 5.0 Comparison of Applied Stress Intensity Factor with the Available Toughness

Stress intensity calculations were performed as a function of crack depth for different times during the transient. The polynomial fit technique described earlier was used for calculating the stress intensity factor due to the combination of thermal and residual stresses. A cubic polynomial was fitted to the stress profile and the magnification factors corresponding to a circumferential crack were used. For pressure stresses, the solution for a finite length crack was used. The total applied stress intensity factor at three different times are shown in Figure 5. The highest stress intensity factors occurred at 300 seconds after the LOCA. The stress intensity factor increased with crack depth reaching a maximum value and then starts decreasing. This is due to the fact that as crack depth increases, the influence of the compressive stress becomes more significant. The material fracture toughness was calculated knowing the crack tip temperature and the local $RT_{NDT}$ after accounting for the fluence effects. For the present problem the temperature was high enough to assure a minimum toughness of 200 ksi $\sqrt{in}$ during the entire transient. From the comparison, it is seen that even with large initial flaws with depth approaching the wall thickness, the fracture toughness for initiation exceeds the applied stress intensity factor by a significant margin. Therefore, an existing flaw in the vessel would not propagate due to brittle fracture during a LOCA.

## 6. CONCLUSIONS

Very conservative assumptions have been made in all phases of the present analysis (particularly in the areas of heat transfer, stress intensity factor calculation and toughness evaluaton). Consequently, the results obtained here provide an upper bound on the applied stress intensity factor, lower bound on the toughness and underestimate the safety margin. Based on this bounding approach, it is concluded that the catastrophic failure of the pressure vessel due to the design basis LOCA is impossible from a fracture mechanics viewpoint.

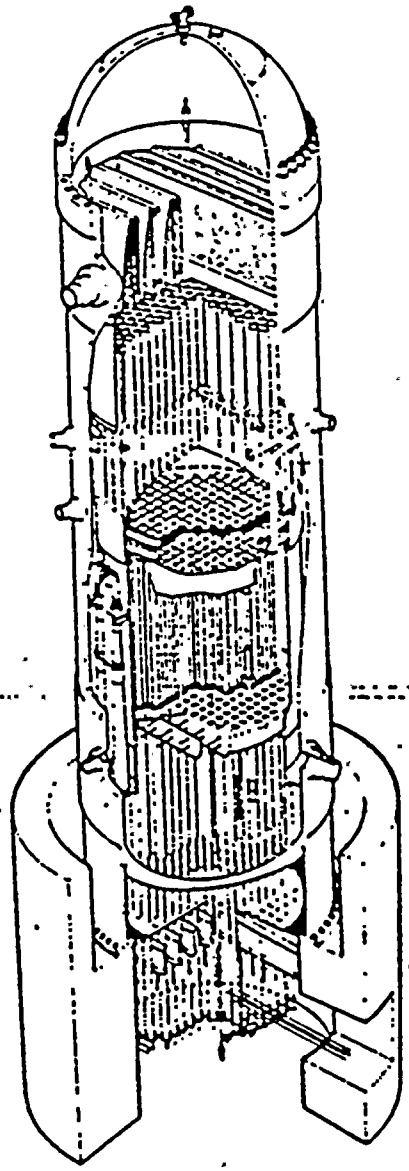

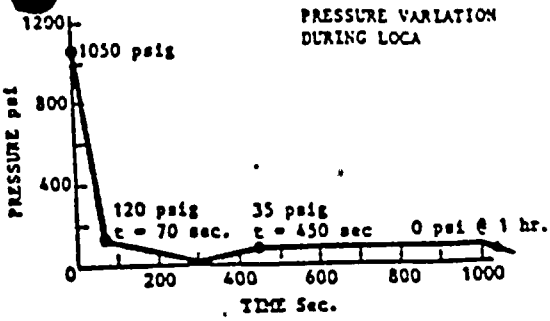


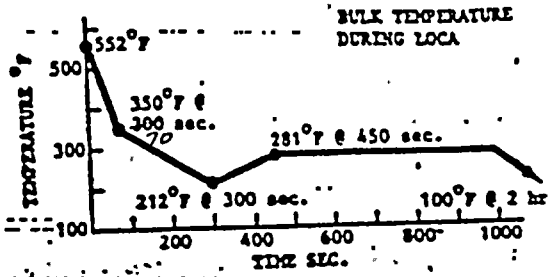


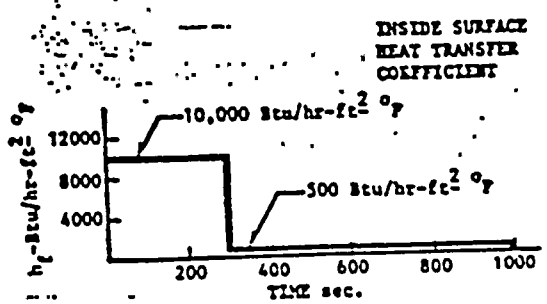


Figure 1. Boiling Water Reactor

Figure 2. Variation of Pressure, Temperature and He
Transfer Coefficient Assumed in the Analy

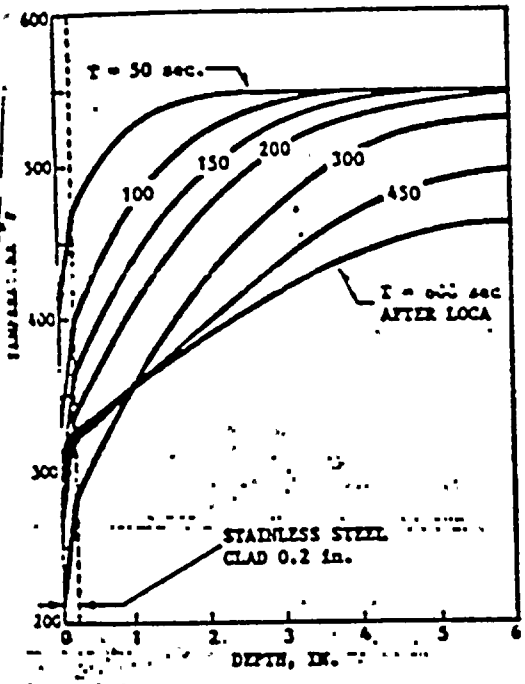


Figure 3. Temperature Distribution in Vessel Wall at Different Times After the Loca.

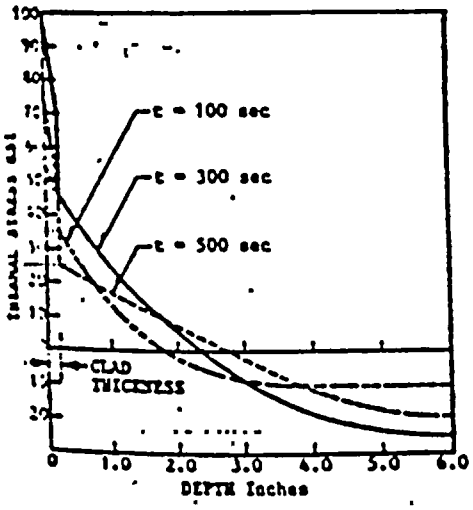


Figure 4. Thermal Stress Distribution at Different Times Following the Loca.

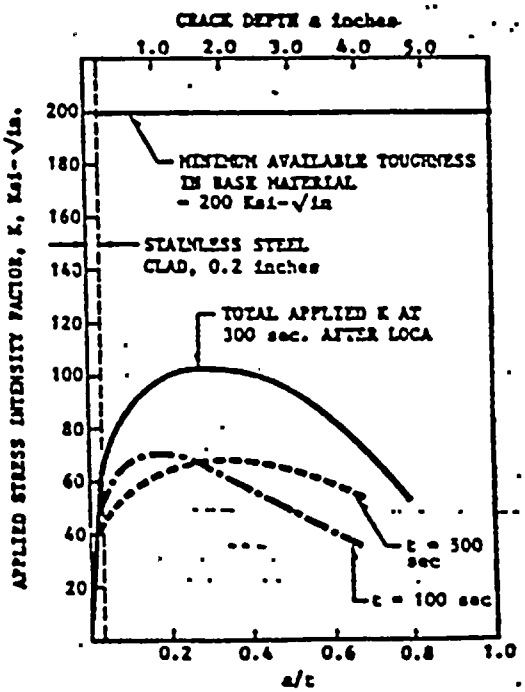


Figure 5. Comparison of Applied Stress Intensity Factors With Available Toughness for Different Crack Depths at Different Times After the Loca.



G 1/5

## ENCES


[1] L. C. Hsu, "An Analytical Study on Brittle Fracture of GE-BWR Vessel Subject to the Design Basis Accident", NEDO-10026, General Electric Company, July 1969.

[2] L. Pujol and A. E. Stenning, "Effect of Flow Direction on the Boiling Heat Transfer Coefficient in Vertical Tubes", Proceedings of an International Symposium on Research in Co-Current Gas-Liquid Flow", held at the University of Waterloo, September 18-19, 1968.

[3] Structural Analysis Program: ANSYS, Swanson Analysis Systems, Inc. Houston, Pennsylvania.

[4] D. A. Ferril, P. E. Juhl and D. E. Miller, "Measurement of Residual Stresses in a Heavy Weldment", Welding Research Supplement 504S to 518S, November 1966.

[5] ASME Boiler and Pressure Vessel Code, Section III, Nuclear Power Plant Components - Division 1, 1974 Edition, American Society of Mechanical Engineers, New York, N.Y.

[6] ASME Boiler and Pressure Vessel Code, Section XI, Rules for Inservice Inspection of Nuclear Power Plant Components, 1974 Edition, American Society of Mechanical Engineers, New York, N.Y.

[7] C. E. Buchalet and W. H. Bamford, "Stress Intensity Factor Solutions for Continuous Surface Flaws in Reactor Pressure Vessels Mechanics of Crack Growth, ASTM STP 590, American Society for Testing and Materials 1976, pp. 385-402.

[8] Regulatory Guide 1.99, Effects of Residual Elements on Predicted Radiation Damage to Reactor Vessel Materials, U.S. Nuclear Regulatory Commission, April 1977 (Revision 1).

ATTACHMENT 3 FOLLOWS

(3 PAGES TOTAL)

NDBH-61
UNIT 1,PAGE 1 08/27/91 16:46:06

HISTORICAL DATA RETRIEVAL AND REVIEW SERVICES
BETWEEN 4:00 ON 1/12/89 AND 8:00 ON 1/12/89
ANALOG DATA

SUBSET:POINT ID'S: NLT01
DATA FOR: 1/12/89

| TIME | POINT ID | POINT DESCRIPTION | STATUS | VALUE | UNITS | LMT EXC |
|---|---|---|---|---|---|---|
| 4:05:27 | NLT01 | RX BOTTOM HEAD DRN TEMP | OK | 516 | DEG F | 2 |
| 4:16:14 | NLT01 | RX BOTTOM HEAD DRN TEMP | OK | 514 | DEG F | 2 |
| 4:16:28 | NLT01 | RX BOTTOM HEAD DRN TEMP | OK | 512 | DEG F | 2 |
| 4:16:54 | NLT01 | RX BOTTOM HEAD DRN TEMP | OK | 509 | DEG F | 2 |
| 4:17:33 | NLT01 | RX BOTTOM HEAD DRN TEMP | OK | 507 | DEG F | 2 |
| 4:17:49 | NLT01 | RX BOTTOM HEAD DRN TEMP | OK | 505 | DEG F | 2 |
| 4:18:03 | NLT01 | RX BOTTOM HEAD DRN TEMP | OK | 503 | DEG F | 2 |
| 4:18:19 | NLT01 | RX BOTTOM HEAD DRN TEMP | OK | 500 | DEG F | 2 |
| 4:18:33 | NLT01 | RX BOTTOM HEAD DRN TEMP | OK | 498 | DEG F | 2 |
| 4:18:48 | NLT01 | RX BOTTOM HEAD DRN TEMP | OK | 496 | DEG F | 2 |
| 4:19:03 | NLT01 | RX BOTTOM HEAD DRN TEMP | OK | 494 | DEG F | 2 |
| 4:19:21 | NLT01 | RX BOTTOM HEAD DRN TEMP | OK | 491 | DEG F | 2 |
| 4:19:41 | NLT01 | RX BOTTOM HEAD DRN TEMP | OK | 489 | DEG F | 2 |
| 4:20:01 | NLT01 | RX BOTTOM HEAD DRN TEMP | OK | 487 | DEG F | 2 |
| 4:20:23 | NLT01 | RX BOTTOM HEAD DRN TEMP | OK | 485 | DEG F | 2 |
| 4:20:45 | NLT01 | RX BOTTOM HEAD DRN TEMP | OK | 482 | DEG F | 2 |
| 4:21:10 | NLT01 | RX BOTTOM HEAD DRN TEMP | OK | 480 | DEG F | 2 |
| 4:21:34 | NLT01 | RX BOTTOM HEAD DRN TEMP | OK | 478 | DEG F | 2 |
| 4:22:01 | NLT01 | RX BOTTOM HEAD DRN TEMP | OK | 476 | DEG F | 2 |
| 4:22:28 | NLT01 | RX BOTTOM HEAD DRN TEMP | OK | 473 | DEG F | 2 |
| 4:22:56 | NLT01 | RX BOTTOM HEAD DRN TEMP | OK | 471 | DEG F | 2 |
| 4:23:25 | NLT01 | RX BOTTOM HEAD DRN TEMP | OK | 469 | DEG F | 2 |
| 4:23:55 | NLT01 | RX BOTTOM HEAD DRN TEMP | OK | 467 | DEG F | 2 |
| 4:24:28 | NLT01 | RX BOTTOM HEAD DRN TEMP | OK | 464 | DEG F | 2 |
| 4:24:55 | NLT01 | RX BOTTOM HEAD DRN TEMP | OK | 462 | DEG F | 2 |
| 4:25:28 | NLT01 | RX BOTTOM HEAD DRN TEMP | OK | 460 | DEG F | 2 |
| 4:26:03 | NLT01 | RX BOTTOM HEAD DRN TEMP | OK | 458 | DEG F | 2 |
| 4:26:35 | NLT01 | RX BOTTOM HEAD DRN TEMP | OK | 455 | DEG F | 2 |
| 4:27:10 | NLT01 | RX BOTTOM HEAD DRN TEMP | OK | 453 | DEG F | 2 |
| 4:27:43 | NLT01 | RX BOTTOM HEAD DRN TEMP | OK | 451 | DEG F | 2 |
| 4:28:25 | NLT01 | RX BOTTOM HEAD DRN TEMP | OK | 449 | DEG F | 2 |
| 4:29:01 | NLT01 | RX BOTTOM HEAD DRN TEMP | OK | 446 | DEG F | 2 |
| 4:29:45 | NLT01 | RX BOTTOM HEAD DRN TEMP | OK | 444 | DEG F | 2 |
| 4:30:28 | NLT01 | RX BOTTOM HEAD DRN TEMP | OK | 442 | DEG F | 2 |
| 4:31:11 | NLT01 | RX BOTTOM HEAD DRN TEMP | OK | 440 | DEG F | 2 |
| 4:31:57 | NLT01 | RX BOTTOM HEAD DRN TEMP | OK | 437 | DEG F | 2 |
| 4:32:39 | NLT01 | RX BOTTOM HEAD DRN TEMP | OK | 435 | DEG F | 2 |
| 4:33:25 | NLT01 | RX BOTTOM HEAD DRN TEMP | OK | 433 | DEG F | 2 |
| 4:34:11 | NLT01 | RX BOTTOM HEAD DRN TEMP | OK | 431 | DEG F | 2 |
| 4:34:57 | NLT01 | RX BOTTOM HEAD DRN TEMP | OK | 428 | DEG F | 2 |
| 4:35:48 | NLT01 | RX BOTTOM HEAD DRN TEMP | OK | 426 | DEG F | 2 |
| 4:36:34 | NLT01 | RX BOTTOM HEAD DRN TEMP | OK | 424 | DEG F | 2 |
| 4:37:25 | NLT01 | RX BOTTOM HEAD DRN TEMP | OK | 422 | DEG F | 2 |
| 4:38:20 | NLT01 | RX BOTTOM HEAD DRN TEMP | OK | 419 | DEG F | 2 |
| 4:39:18 | NLT01 | RX BOTTOM HEAD DRN TEMP | OK | 417 | DEG F | 2 |
| 4:40:13 | NLT01 | RX BOTTOM HEAD DRN TEMP | OK | 415 | DEG F | 2 |
| 4:41:11 | NLT01 | RX BOTTOM HEAD DRN TEMP | OK | 413 | DEG F | 2 |
| 4:42:11 | NLT01 | RX BOTTOM HEAD DRN TEMP | OK | 410 | DEG F | 2 |

NDBH-61
UNIT 1,PAGE 2 08/27/91 16:46:06

HISTORICAL DATA RETRIEVAL AND REVIEW SERVICES
BETWEEN 4:00 ON 1/12/89 AND 8:00 ON 1/12/89
ANALOG DATA

SUBSET:POINT ID'S: NLT01
DATA FOR: 1/12/89

| TIME | POINT ID | POINT DESCRIPTION | STATUS | VALUE | UNITS | LMT EXC |
|---|---|---|---|---|---|---|
| 4:43:15 | NLT01 | RX BOTTOM HEAD DRN TEMP | OK | 408 | DEG F | 2 |
| 4:44:21 | NLT01 | RX BOTTOM HEAD DRN TEMP | OK | 406 | DEG F | 2 |
| 4:45:30 | NLT01 | RX BOTTOM HEAD DRN TEMP | OK | 404 | DEG F | 2 |
| 4:46:39 | NLT01 | RX BOTTOM HEAD DRN TEMP | OK | 401 | DEG F | 2 |
| 4:47:53 | NLT01 | RX BOTTOM HEAD DRN TEMP | OK | 399 | DEG F | 2 |
| 4:49:11 | NLT01 | RX BOTTOM HEAD DRN TEMP | OK | 397 | DEG F | 2 |
| 4:50:25 | NLT01 | RX BOTTOM HEAD DRN TEMP | OK | 395 | DEG F | 2 |
| 4:51:45 | NLT01 | RX BOTTOM HEAD DRN TEMP | OK | 392 | DEG F | 2 |
| 4:53:06 | NLT01 | RX BOTTOM HEAD DRN TEMP | OK | 390 | DEG F | 2 |
| 4:54:30 | NLT01 | RX BOTTOM HEAD DRN TEMP | OK | 388 | DEG F | 2 |
| 4:55:56 | NLT01 | RX BOTTOM HEAD DRN TEMP | OK | 386 | DEG F | 2 |
| 4:57:31 | NLT01 | RX BOTTOM HEAD DRN TEMP | OK | 383 | DEG F | 2 |
| 4:59:27 | NLT01 | RX BOTTOM HEAD DRN TEMP | OK | 381 | DEG F | 2 |
| 5:03:41 | NLT01 | RX BOTTOM HEAD DRN TEMP | OK | 383 | DEG F | 2 |
| 5:04:10 | NLT01 | RX BOTTOM HEAD DRN TEMP | OK | 386 | DEG F | 2 |
| 5:04:38 | NLT01 | RX BOTTOM HEAD DRN TEMP | OK | 388 | DEG F | 2 |
| 5:05:00 | NLT01 | RX BOTTOM HEAD DRN TEMP | OK | 390 | DEG F | 2 |
| 5:05:18 | NLT01 | RX BOTTOM HEAD DRN TEMP | OK | 392 | DEG F | 2 |
| 5:05:31 | NLT01 | RX BOTTOM HEAD DRN TEMP | OK | 395 | DEG F | 2 |
| 5:05:49 | NLT01 | RX BOTTOM HEAD DRN TEMP | OK | 397 | DEG F | 2 |
| 5:06:10 | NLT01 | RX BOTTOM HEAD DRN TEMP | OK | 399 | DEG F | 2 |
| 5:06:26 | NLT01 | RX BOTTOM HEAD DRN TEMP | OK | 401 | DEG F | 2 |
| 5:06:45 | NLT01 | RX BOTTOM HEAD DRN TEMP | OK | 404 | DEG F | 2 |
| 5:07:08 | NLT01 | RX BOTTOM HEAD DRN TEMP | OK | 406 | DEG F | 2 |
| 5:07:30 | NLT01 | RX BOTTOM HEAD DRN TEMP | OK | 408 | DEG F | 2 |
| 5:07:53 | NLT01 | RX BOTTOM HEAD DRN TEMP | OK | 410 | DEG F | 2 |
| 5:08:25 | NLT01 | RX BOTTOM HEAD DRN TEMP | OK | 413 | DEG F | 2 |
| 5:09:05 | NLT01 | RX BOTTOM HEAD DRN TEMP | OK | 415 | DEG F | 2 |
| 5:10:03 | NLT01 | RX BOTTOM HEAD DRN TEMP | OK | 417 | DEG F | 2 |
| 5:11:57 | NLT01 | RX BOTTOM HEAD DRN TEMP | OK | 419 | DEG F | 2 |
| 5:15:25 | NLT01 | RX BOTTOM HEAD DRN TEMP | OK | 417 | DEG F | 2 |
| 5:19:01 | NLT01 | RX BOTTOM HEAD DRN TEMP | OK | 415 | DEG F | 2 |
| 5:20:28 | NLT01 | RX BOTTOM HEAD DRN TEMP | OK | 417 | DEG F | 2 |
| 5:20:31 | NLT01 | RX BOTTOM HEAD DRN TEMP | OK | 419 | DEG F | 2 |
| 5:20:35 | NLT01 | RX BOTTOM HEAD DRN TEMP | OK | 422 | DEG F | 2 |
| 5:20:40 | NLT01 | RX BOTTOM HEAD DRN TEMP | OK | 425 | DEG F | 2 |
| 5:20:43 | NLT01 | RX BOTTOM HEAD DRN TEMP | OK | 427 | DEG F | 2 |
| 5:20:48 | NLT01 | RX BOTTOM HEAD DRN TEMP | OK | 429 | DEG F | 2 |
| 5:20:53 | NLT01 | RX BOTTOM HEAD DRN TEMP | OK | 431 | DEG F | 2 |
| 5:20:58 | NLT01 | RX BOTTOM HEAD DRN TEMP | OK | 434 | DEG F | 2 |
| 5:21:05 | NLT01 | RX BOTTOM HEAD DRN TEMP | OK | 436 | DEG F | 2 |
| 5:21:13 | NLT01 | RX BOTTOM HEAD DRN TEMP | OK | 438 | DEG F | 2 |
| 5:21:23 | NLT01 | RX BOTTOM HEAD DRN TEMP | OK | 440 | DEG F | 2 |
| 5:21:41 | NLT01 | RX BOTTOM HEAD DRN TEMP | OK | 443 | DEG F | 2 |
| 5:22:31 | NLT01 | RX BOTTOM HEAD DRN TEMP | OK | 445 | DEG F | 2 |
| 5:24:13 | NLT01 | RX BOTTOM HEAD DRN TEMP | OK | 443 | DEG F | 2 |
| 5:26:53 | NLT01 | RX BOTTOM HEAD DRN TEMP | OK | 440 | DEG F | 2 |
| 5:28:43 | NLT01 | RX BOTTOM HEAD DRN TEMP | OK | 438 | DEG F | 2 |

NDBH-61
UNIT 1,PAGE 3 08/27/91 16:46:06

HISTORICAL DATA RETRIEVAL AND REVIEW SERVICES
BETWEEN 4:00 ON 1/12/89 AND 8:00 ON 1/12/89
ANALOG DATA

SUBSET:POINT ID'S: NLT01
DATA FOR: 1/12/89

| TIME | POINT ID | POINT DESCRIPTION | STATUS | VALUE | UNITS | LMT EXC |
|---|---|---|---|---|---|---|
| 5:30:51 | NLT01 | RX BOTTOM HEAD DRN TEMP | OK | 436 | DEG F | 2 |
| 5:33:04 | NLT01 | RX BOTTOM HEAD DRN TEMP | OK | 434 | DEG F | 2 |
| 5:35:28 | NLT01 | RX BOTTOM HEAD DRN TEMP | OK | 431 | DEG F | 2 |
| 5:37:53 | NLT01 | RX BOTTOM HEAD DRN TEMP | OK | 429 | DEG F | 2 |
| 5:40:15 | NLT01 | RX BOTTOM HEAD DRN TEMP | OK | 427 | DEG F | 2 |
| 5:42:25 | NLT01 | RX BOTTOM HEAD DRN TEMP | OK | 425 | DEG F | 2 |
| 5:44:37 | NLT01 | RX BOTTOM HEAD DRN TEMP | OK | 422 | DEG F | 2 |
| 5:46:48 | NLT01 | RX BOTTOM HEAD DRN TEMP | OK | 420 | DEG F | 2 |
| 5:49:15 | NLT01 | RX BOTTOM HEAD DRN TEMP | OK | 418 | DEG F | 2 |
| 5:55:21 | NLT01 | RX BOTTOM HEAD DRN TEMP | OK | 416 | DEG F | 2 |
| 5:59:49 | NLT01 | RX BOTTOM HEAD DRN TEMP | OK | 413 | DEG F | 2 |
| 6:05:31 | NLT01 | RX BOTTOM HEAD DRN TEMP | OK | 411 | DEG F | 2 |
| 6:11:51 | NLT01 | RX BOTTOM HEAD DRN TEMP | OK | 409 | DEG F | 2 |
| 6:18:45 | NLT01 | RX BOTTOM HEAD DRN TEMP | OK | 407 | DEG F | 2 |
| 6:33:58 | NLT01 | RX BOTTOM HEAD DRN TEMP | OK | 404 | DEG F | 2 |
| 6:55:33 | NLT01 | RX BOTTOM HEAD DRN TEMP | OK | 402 | DEG F | 2 |
| 7:14:51 | NLT01 | RX BOTTOM HEAD DRN TEMP | OK | 400 | DEG F | 2 |
| 7:32:35 | NLT01 | RX BOTTOM HEAD DRN TEMP | OK | 398 | DEG F | 2 |
| 7:47:39 | NLT01 | RX BOTTOM HEAD DRN TEMP | OK | 395 | DEG F | 2 |

* * * E N D O F D A T A * * *

ATTACHMENT 4 FOLLOWS

(5 PAGES TOTAL)